

## THE RELATION BETWEEN COMPACT, QUIESCENT HIGH REDSHIFT GALAXIES AND MASSIVE NEARBY ELLIPTICAL GALAXIES: EVIDENCE FOR HIERARCHICAL, INSIDE-OUT GROWTH

RACHEL BEZANSON<sup>1</sup>, PIETER G. VAN DOKKUM<sup>1</sup>, TOMER TAL<sup>1</sup>, DANILO MARCHESE<sup>1</sup>, MARISKA KRIEK<sup>2</sup>, MARIJN FRANX<sup>3</sup> AND PAOLO COPPI<sup>1</sup>*Accepted for publication in the Astrophysical Journal*

## ABSTRACT

Recent studies have shown that massive quiescent galaxies at high redshift are much more compact than present-day galaxies of the same mass. Here we compare the radial stellar density profiles and the number density of a sample of massive galaxies at  $z \sim 2.3$  to nearby massive elliptical galaxies. We confirm that the average stellar densities of the  $z \sim 2.3$  galaxies within the effective radius,  $\rho(< r_e)$ , are two orders of magnitude higher than those of local elliptical galaxies of the same stellar mass. However, we also find that the densities measured within a constant physical radius of 1 kpc,  $\rho(< 1 \text{ kpc})$ , are higher by a factor of 2–3 only. This suggests that inside-out growth scenarios are plausible, in which the compact high redshift galaxies make up the centers of normal nearby ellipticals. The compact galaxies are common at high redshift, which enables us to further constrain their evolution by requiring that the number density of their descendants does not exceed constraints imposed by the  $z = 0$  galaxy mass function. We infer that size growth must be efficient, with  $(r_{1+2}/r_1) \sim (M_{1+2}/M_1)^2$ . A simple model where compact galaxies with masses  $\sim 10^{11} M_\odot$  primarily grow through minor mergers produces descendants with the approximate sizes, stellar densities, and number density of elliptical galaxies with masses  $2–3 \times 10^{11} M_\odot$  in the local Universe. We note that this model also predicts evolution in the  $M_{\text{BH}} - \sigma$  relation, such that the progenitors of elliptical galaxies have lower black hole masses at fixed velocity dispersion. The main observational uncertainty is the conversion from light to mass; measurements of kinematics are needed to calibrate the masses and stellar densities of the high redshift galaxies.

*Subject headings:* cosmology: observations — galaxies: evolution — galaxies: formation — galaxies: elliptical and lenticular, cD

## 1. INTRODUCTION

Several recent studies have found that the oldest and most massive galaxies at high redshift have very small sizes (e.g., Trujillo et al. 2006; Daddi et al. 2005; Toft et al. 2007; Zirm et al. 2007; van Dokkum et al. 2008; Cimatti et al. 2008; van der Wel et al. 2008; Franx et al. 2008; Damjanov et al. 2008; Buitrago et al. 2008). Although these studies use different datasets and methodology they are in good agreement, finding that the effective radii of red, apparently quiescent galaxies of fixed mass evolved by a factor of  $\sim 5$  since  $z \sim 2.5$  (e.g., van der Wel et al. 2008). Initially there were concerns about the quality of photometric redshifts, the depth of the imaging data, and the interpretation of the broad-band spectral energy distributions (SEDs), but these were recently addressed through deep Gemini/GNIRS near-infrared spectroscopy and deep HST/NICMOS imaging of a sample of massive quiescent galaxies at  $z \sim 2.3$  (Kriek et al. 2006; van Dokkum et al. 2008).

These small galaxies are remarkable when compared to nearby galaxies, as their average stellar densities are a factor of  $\gtrsim 100$  higher than those of red SDSS galaxies of the same mass (van Dokkum et al. 2008). Such massive, dense galaxies are very rare in the local Universe (e.g., Trujillo et al. 2009) but they make up about half of galaxies with  $M \gtrsim 10^{11} M_\odot$  at  $z \sim 2.3$  (e.g., van Dokkum et al. 2006; Kriek et al. 2006; Williams et al. 2008).

Various scenarios have been proposed to explain the observed properties of the compact galaxies and to describe their subsequent evolution. The most straightforward explanation is that the masses are overestimated and/or the sizes underestimated. The mass measurements currently rely on fitting stellar population synthesis models to the observed photometry and spectra, and these models have considerable systematic uncertainties. A significant uncertainty is the stellar initial mass function (IMF): a “bottom-light” IMF, such as proposed by, e.g., van Dokkum (2008), Davé (2008), and Wilkins, Trentham, & Hopkins (2008), would generally lower the implied masses, with the precise effect depending on the age of the stellar populations. The sizes of the galaxies can be underestimated in several ways. It may be that the galaxies have strong radial gradients in  $M/L$  ratio, in which case the luminosity-weighted sizes are different from the mass-weighted sizes (e.g., Hopkins et al. 2008). We also note that Hopkins et al. (2008) predict smaller differences between nearby elliptical galaxies and their progenitors, due to contribution of the dark matter halos. Limitations in resolution and signal-to-noise ratio may also play a role, although this seems increasingly unlikely.

Taking the measured masses and sizes at face value, three effects have been discussed to explain the observed evolution. The first is a variation on “progenitor bias” (van Dokkum & Franx 2001), which states that early-type galaxies at high redshift are only a subset of all progenitors of today’s early-type galaxies. As we discuss later, the number density of the compact galaxies at  $z \sim 2.3$  is only  $\sim 7\%$  of the number density of galaxies with the same mass today (see § 5.1)<sup>4</sup>. Therefore, the

<sup>1</sup> Department of Astronomy, Yale University, New Haven, CT 06520-8101<sup>2</sup> Department of Astrophysical Sciences, Princeton University, Princeton, NJ 08544<sup>3</sup> Sterrewacht Leiden, Leiden University, NL-2300 RA Leiden, Netherlands<sup>4</sup> We note that this fraction is smaller than that found in Kriek et al. (2008).

compact galaxies may be the progenitors of the most compact  $\sim 7\%$  of today's galaxies with the same mass (see also Franx et al. 2008). This explanation cannot be complete, as the compact galaxies are small even when compared to this subset of the present-day population. The second explanation is minor or major merging, which will increase the sizes but also the masses (Khochfar & Silk 2006; Naab et al. 2007; Hopkins et al. 2008). Significant merging is expected for these massive galaxies, e.g., White et al. (2007); Guo & White (2008), and merging scenarios have been discussed in several papers (e.g., Cimatti et al. 2008; van der Wel et al. 2008). The third explanation that has been discussed is expansion of the galaxies as a result of dramatic mass loss due to quasar feedback (Fan et al. 2008).

In this paper we provide new constraints on the evolution of compact "red and dead" high redshift galaxies. In § 3 we compare the radial stellar density profiles of the compact galaxies to those of nearby elliptical galaxies. This allows us to determine whether the compact galaxies resemble the central regions of elliptical galaxies, and hence whether normal elliptical galaxies are plausible descendants via merging scenarios. In § 4 we present three simple models to explain the growth of compact galaxies into local elliptical galaxies. In § 5 we consider which of the modes is most likely to dominate galaxy growth by including constraints from the evolution of the mass function, and derive a lower bound on the amount of size growth for a given amount of mass growth. Throughout this paper, we assume a  $\Lambda$ CDM cosmology with  $H_0 = 70 \text{ km s}^{-1} \text{ Mpc}^{-1}$ ,  $\Omega_m = 0.3$ , and  $\Omega_\Lambda = 0.7$ .

## 2. DENSITY PROFILES

Density profiles of nearby elliptical galaxies and the compact high redshift galaxies are constructed. For the compact galaxies we deproject the Sersic fits presented in vD08, and for the nearby galaxies we use a combination of new and literature data.

### 2.1. Surface Brightness Profiles

#### 2.1.1. High Redshift Galaxies

We use the sample of nine high redshift "red and dead" galaxies previously studied by Kriek et al. (2006) and van Dokkum et al. (2008) [hereafter vD08]. The redshifts of the galaxies were measured from deep rest-frame optical Gemini/GNIRS spectra (Kriek et al. 2006). The spectra also demonstrate that the light comes from evolved stellar populations, as they exhibit prominent Balmer or 4000 Å breaks. The galaxies were imaged with the Hubble Space Telescope (HST) NICMOS2 camera, and with Keck/NIRC2 using laser guide star-assisted adaptive optics. As described in vD08, the galaxies were fit with Sersic (1968) profiles using GALFIT (Peng et al. 2002). Structural parameters for the galaxies are listed in vD08.

Surface brightness profiles in the  $H_{160}$  band were constructed from the Sersic fits. The galaxies are barely resolved even with the NICMOS2 camera, and we have essentially no information on the form of the density profile within the effective radius ( $0.^{\prime\prime}1$ , or  $\approx 1$  kpc). The average density within this radius is much better constrained, and this is the parameter that we will use in quantitative comparisons. We note

The reason is that we adopt a different IMF and therefore a different mass limit, and we assume that at  $z = 0$  all galaxies with  $M \geq 10^{11} M_\odot$  are "red and dead" but only  $\sim 50\%$  at  $z = 2.5$ .

that GALFIT effectively extrapolates the Sersic fits to the (resolved) structure at large radii inward while conserving the total flux, and that therefore the fits *may* also provide a good approximation of the form of the density profile within 1 kpc.

#### 2.1.2. Nearby Galaxies

Two sources are used for the nearby sample. The Tal, van Dokkum, & Nelan (2009) [hereafter T09] sample is an absolute magnitude and volume-limited sample of local elliptical galaxies, selected from Tully (1988). All galaxies with morphological type "E",  $M_B < -20$ , within declinations of  $-85$  and  $+10$ , galactic latitude  $> 17^\circ$  or  $< -17^\circ$  and at distances of  $15-50$  Mpc were observed with the Yale 1.0 m telescope at CTIO, operated by the SMARTS consortium, in the  $V$  band. The observing strategy was optimized for flat-fielding accuracy, and the surface brightness profiles can be reliably traced to  $\approx 29$  mag arcsec $^{-2}$ . The galaxies were fit with isophotal ellipses using IRAF. Apparent magnitudes were calibrated using aperture photometry of Prugniel & Heraudeau (1998) and then converted to  $B$  magnitudes using published  $B-V$  colors from the same catalogue (neglecting color gradients). Measurements were corrected for Galactic reddening using infrared dust maps from Schlegel, Finkbeiner, & Davis (1998). We assume distance measurements from the Tully catalogue (corrected to our cosmology) to convert the luminosity profiles to physical units.

The T09 sample has the advantage that it is complete down to a luminosity limit (which roughly corresponds to a mass limit for these luminous red ellipticals), but the disadvantage is that it only samples a limited range in mass and luminosity. We supplemented the T09 sample with photometry from Franx, Illingworth, & Heckman (1989); Peletier et al. (1990); Jedrzejewski (1987) [hereafter FPJ]. This sample is not complete but covers a larger range in luminosity. We limited the sample to all galaxies that have published  $B$ -band profiles. Again distances from Tully (1988) were used to convert the observed brightnesses to luminosities.

#### 2.2. Deprojection

The intensity profiles of the nearby galaxies are fit to Sersic profiles of the form

$$I(r) = I_o \exp \left[ -b_n \left( \frac{r}{r_e} \right)^{1/n} \right] \quad (1)$$

with  $n \leq 4$  between radii of  $4''$  out to 20 kpc, or the maximum extent of each profile, along the circularized axis,  $r = a\sqrt{1-\epsilon}$ , of the galaxy (Ciotti 1991).  $b_n$  is defined as the solution to  $\gamma(2n, b_n) = \Gamma(2n)/2$ . We use the asymptotic approximation for  $b_n$ , which is accurate to a factor of  $\mathcal{O} \sim 10^{-6}$ :

$$b_n \approx 2n - \frac{1}{3} + \frac{4}{405n} + \frac{46}{25515n^2} \quad (2)$$

(Ciotti & Bertin 1999). For the high redshift galaxies we used the fits of vD08. We then performed an Abel Transform to deproject a circularized, three-dimensional light profile:

$$\rho_L \left( \frac{r}{r_e} \right) = \frac{b_n I_o}{\pi r_e} \left( \frac{r}{r_e} \right)^{(1/n-1)} \int_1^\infty \frac{\exp[-b_n(\frac{r}{r_e})^{(1/n)}t]}{\sqrt{t^{2n}-1}} dt \quad (3)$$

For both the high redshift sample of compact galaxies and the two samples of nearby elliptical galaxies we now have circularized radial luminosity density profiles in units of  $L_{B,\odot} \text{ kpc}^{-3}$ .

### 2.3. Light-to-Mass Conversions

In order to convert the luminosity density profiles to stellar mass density profiles we make the following assumptions about the mass-to-light ( $M/L$ ) ratios. For the high redshift sample we use stellar masses from Kriek et al. (2008) adjusted to a Kroupa (2001) IMF. For the nearby sample, we use the well-established relation between  $M/L$  ratio and mass to convert luminosities to masses (e.g., van der Marel 1991). The normalization and slope of the relation in the  $B$  band were determined by combining the information in Table 1 of van der Marel (1991) and Table 2 in van der Marel & van Dokkum (2007):

$$\frac{M}{L_B} = (9.04 \times 10^{-4}) \left( \frac{L_B}{L_{B,\odot}} \right)^{0.37} \quad (4)$$

The conversion from luminosity to mass is the largest uncertainty in the methodology, in particular the lack of dynamical measurements that could calibrate the  $M/L$  ratios of the high redshift galaxies. We will return to this issue in § 6.

## 3. COMPARISON OF DENSITY PROFILES

### 3.1. Average Profiles

The stellar density profiles of the compact high redshift galaxies are compared to those of nearby elliptical galaxies in Fig. 1. The solid line is the average density profile of the 9 galaxies from vD08. We use a 1000 iteration bootstrap estimation to approximate errors of the average density profile due to the small sample size of the high redshift galaxies. The  $1\sigma$  contour is shown in dark gray and the  $2\sigma$  is shown in light gray. Broken lines are average profiles of nearby elliptical galaxies from the T09 sample, in three different mass bins. The lowest mass bin is  $M \geq 10^{11} M_\odot$ : this is the mass that the high redshift galaxies already have at the epoch of observation, and therefore the minimum mass of their descendants.

Figure 1 shows that the discrepancy between the profiles of compact high redshift galaxies and nearby elliptical galaxies is mostly in the outer regions. Within  $r \approx 1$  kpc the average stellar density of the high redshift galaxies is greater than the density of nearby ellipticals by a factor of a few only, particularly for the more massive galaxies in the T09 sample. This discrepancy is much smaller than the factor of  $\gtrsim 100$  difference when the density is measured within the effective radius (e.g., vD08). Furthermore, our error estimates only address the sample bias; this discrepancy is especially small considering the other sources of uncertainty in our measurements, which we will discuss further in § 6. Outside of this inner region, the difference grows significantly; the stellar density of nearby elliptical galaxies is a few hundred times higher than that of the compact high redshift galaxies at  $r > 10$  kpc. We infer that in order to evolve into nearby galaxies, compact galaxies need not change significantly in the central regions, but must grow significantly in their outer regions.

### 3.2. Comparison of Masses, Sizes, and Densities

The relative properties of the high redshift galaxies and nearby galaxies are demonstrated in Figure 2. The compact galaxies from vD08 are indicated by solid circles. The nearby samples are represented by open symbols: squares for T09 and triangles for FPJ. Only nearby galaxies with sufficient mass,  $M \gtrsim 10^{11} M_\odot$ , can be the descendants of the high redshift galaxies. Galaxies with lower masses are denoted with light grey symbols.

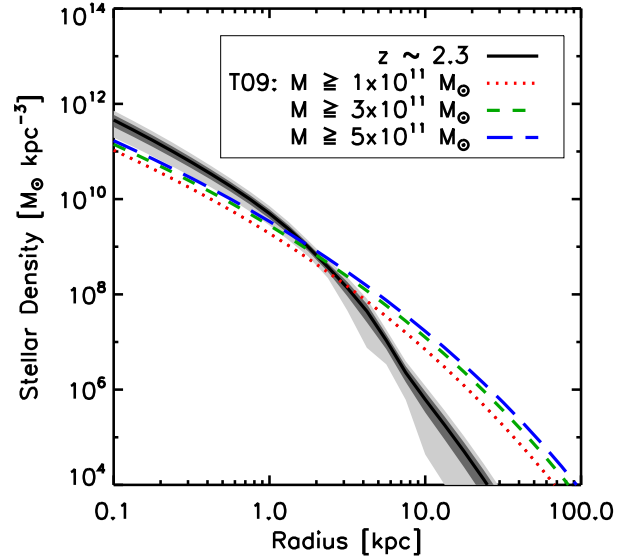


FIG. 1.— Comparison of the mean stellar density profiles of high redshift compact galaxies (solid line) with nearby elliptical galaxies from the T09 sample (broken lines). High redshift 1 and  $2\sigma$  contours are shown in gray. The average density profile for nearby galaxies with  $M \geq 10^{11} M_\odot$  is represented by the red, dashed line; the green, short dashed line corresponds to galaxies with  $M \geq 3 \times 10^{11} M_\odot$ ; and the most massive local galaxies with  $M \geq 5 \times 10^{11} M_\odot$  are shown by the blue, long-dashed line. Note that the profiles of the nearby galaxies are fairly similar to those of the compact galaxies at radii  $r \lesssim 3$  kpc, qualitatively consistent with expectations for inside-out growth.

The relative compactness of high redshift and low redshift galaxies is shown in Figure 2(a). There is a clear trend showing the increasing effective radius with galaxy mass in the nearby galaxies. The high redshift galaxies, though in the middle of the nearby mass range, are smaller by a factor of  $\sim 5$  in effective radius. This result confirms previous studies, which generally used the Sloan Digital Sky Survey (SDSS) as a low redshift comparison point (e.g., Toft et al. 2007; van Dokkum et al. 2008; Cimatti et al. 2008; van der Wel et al. 2008). van der Wel et al. (2008) combine data from the literature (in addition to adding new data at  $z \approx 1$ ) and derive an evolution of  $r_e \propto (1+z)^{-1.20 \pm 0.12}$  at fixed mass (for samples with photometrically determined masses), corresponding to a factor of  $4.2 \pm 0.6$  at  $z = 2.3$ .

The difference in size at fixed mass implies a significant difference in density contained within the effective radius of the high redshift and nearby galaxies. We calculated the average densities within the effective radius by integrating the stellar density profiles derived in the previous Section:

$$\rho(< r) = \frac{3}{r^3} \int_0^r \rho(r') r'^2 dr' \quad (5)$$

with  $r = r_e$ . This difference is obvious in Figure 2(b): the vertical axis of this panel demonstrates the factor of  $> 100$  differences in the average density within the effective radius.

The horizontal axis of Fig. 2(b) shows the average density integrated to  $r = 1$  kpc rather than  $r = r_e$ . For convenience, we will refer to the average density within 1 kpc as the “central density”. Since the compact galaxies have effective radii  $\sim 1$  kpc, the density within  $r_e$  is approximately equivalent to our definition of the central density, placing these galaxies along the dashed diagonal line representing the equality of the two densities. The nearby sample lies predominantly be-

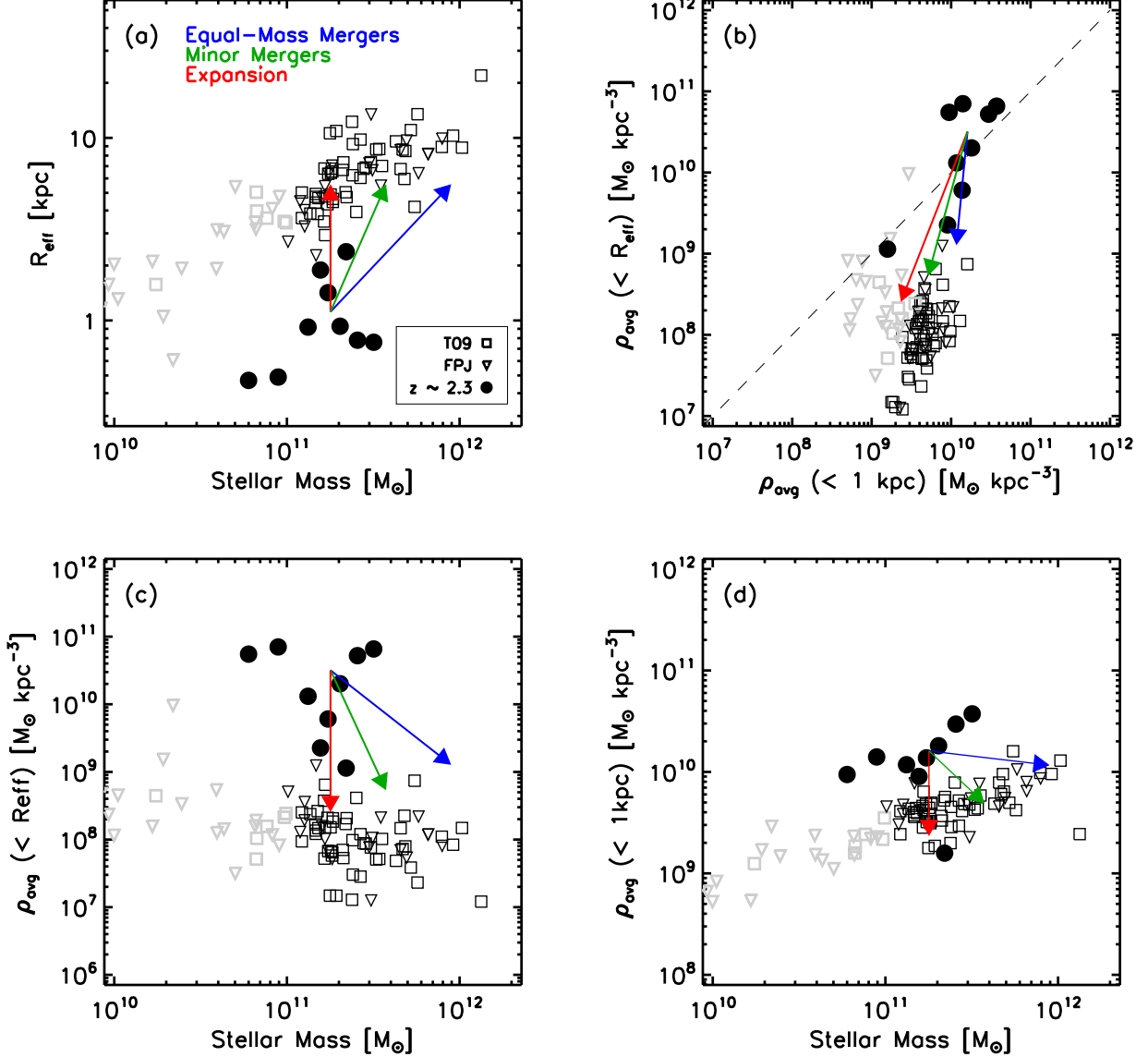


FIG. 2.— Relative properties of nearby and  $z \sim 2.3$  galaxies. The panels show the relations between size and mass (a), density within the effective radius and density within 1 kpc (b), density within the effective radius and mass (c), and density within 1 kpc and mass (d). Open symbols are nearby galaxies, solid circles are high redshift compact galaxies from vD08. Light grey points are nearby galaxies with masses  $< 10^{11} M_{\odot}$ , i.e., lower than the high  $z$  compact galaxies. Arrows begin at mean values of high redshift sample and show predictions from simple models for the evolution of the compact galaxies: blue arrows shows the direction of evolution due to equal-mass mergers, green arrows for minor mergers and red arrows for the expansion model. Simple expansion or equal-mass mergers can bring the distant galaxies close to the scaling relations defined by nearby galaxies, but equal-mass mergers do not produce galaxies of the right size.

low this line, with  $\rho(< r_e)$  much lower than  $\rho(< 1 \text{ kpc})$  for all galaxies with masses  $> 10^{11} M_{\odot}$ . We infer that, although the high redshift galaxies have higher densities than nearby ellipticals overall, the differences are much smaller within 1 kpc than within  $1 r_e$ .

Figure 2(c) and (d) demonstrate the same point in the density versus mass plane. In (c), we show the relation between  $\rho(< r_e)$  and total stellar mass. The compact high redshift galaxies are clearly much denser than nearby galaxies of the same mass. In (d), it is shown that the discrepancy in density becomes far less extreme in the central regions of the galaxies. The nearby sample shows opposite trends with mass in (c) and (d): the density within the effective radius decreases with increasing mass (reflecting the slope of the mass – radius relation), but the density within 1 kpc grows with increasing

mass. Interestingly, the central densities of the high redshift compact galaxies are very similar to those of nearby elliptical galaxies with masses  $\gtrsim 5 \times 10^{11} M_{\odot}$ .

The trends in Fig. 2 are consistent with models in which the compact galaxies make up the centers of present-day giant ellipticals. Such inside-out formation scenarios are not new, and have been explored by, e.g., Loeb & Peebles (2003), Bournaud, Jog, & Combes (2007), Naab et al. (2007), and Hopkins et al. (2008). The idea is that a compact core is formed through highly dissipative processes at  $z \gtrsim 3$  (see, e.g., Robertson et al. 2006a; Dekel et al. 2008), which then grows through increasingly dissipationless mergers at lower redshift. Independently, Franx et al. 2008 argues that galaxy growth is mostly inside-out, based both on the regular evolution of the stellar mass-radius relation, and on the fact that star forming

galaxies are larger than non-star forming galaxies of the same mass.

#### 4. PREDICTIONS FROM SIMPLE MODELS

As discussed in § 1, various models have been proposed to explain the apparent growth of massive galaxies since  $z \sim 2.5$ . Here we discuss three possible simple models in the context of the relations shown in Fig. 2: equal-mass mergers, minor mergers and expansion at fixed mass. We investigate the effects of these models in Fig. 2 with arrows. The starting point of the arrows is always the mean of the high redshift compact galaxies, and they all imply a growth in effective radius of a factor of 5. We emphasize that we look to constrain the dominant mode of galaxy evolution; while individual galaxies in the sample will likely be affected by all of the processes discussed below, we focus on the overall trends in the larger context of the sample of galaxies.

##### 4.1. Model 1: Growth via Equal-Mass Mergers

In this model, the growth is driven by (near-) equal mass mergers. These mergers will not only increase the size of the galaxies, but also their mass. Applying straightforward virial arguments implies

$$K_{1+2} = K_1 + K_2, \quad (6)$$

with  $K_{1+2}$  the kinetic energy of the remnant and  $K_1, K_2$  the kinetic energy of the progenitors. With  $K = \frac{1}{2}M\sigma^2$  we have

$$\frac{1}{2}M_{1+2}\sigma_{1+2}^2 = \frac{1}{2}M_1\sigma_1^2 + \frac{1}{2}M_2\sigma_2^2, \quad (7)$$

and as  $M_{1+2} = M_1 + M_2$  and  $M_1 = M_2$ , we have  $\sigma_{1+2}^2 = \sigma_1^2$ . Using  $\sigma^2 \propto GM/r$ , we arrive at

$$\frac{r_{1+2}}{r_1} = \frac{M_{1+2}}{M_1}, \quad (8)$$

the familiar result that mergers lead to an increase in size and mass but no change in velocity dispersion (e.g., Barnes 1992). We note that these relations are simplifications, which are inconsistent with the observed slopes of the stellar mass – radius relation and the stellar mass –  $\sigma$  relation. Simulations which take the initial orbits and effects of energy transfer to the dark matter halos into account generally imply a smaller increase in size for a given change in mass. Boylan-Kolchin, Ma, & Quataert (2006) find that  $r_{1+2}/r_1 \sim (M_{1+2}/M_1)^{0.6-1}$ , depending on the orbital configuration.

The blue arrows in Fig. 2(a-d) show the effects of equal-mass mergers on the various relations between mass, size, and density. The density within 1 kpc was calculated by assuming that the Sersic indices of the profiles of the compact galaxies do not change. The blue arrows imply that the descendants of the compact galaxies are the dominant galaxies in massive groups and clusters, with stellar masses of  $\sim 10^{12} M_\odot$ . As can be seen in panel *d*, the central densities of these galaxies are nearly identical to those of the compact galaxies. However, as can be seen in panel *a*, the effective radii of these giant, nearby galaxies are a factor of  $\sim 10$  larger than the compact objects, not a factor of  $\sim 5$ . Therefore, this model is not a very good description of the required evolution in panels *a* – *c*.

##### 4.2. Model 2: Growth via Minor Mergers

In this mode of galaxy growth, the progenitor galaxies accumulate mass via minor mergers with small systems. The

difference with the equal-mass merger model is that minor mergers are more effective in “puffing up” the size a galaxy for a given change in stellar mass. For minor mergers  $\sigma_1^2 \gg \sigma_2^2$  in Eq. 7, and therefore

$$\frac{\sigma_{1+2}^2}{\sigma_1^2} \approx \frac{M_1}{M_{1+2}} \quad (9)$$

Again using  $\sigma^2 \propto GM/r$  we have

$$\frac{r_{1+2}}{r_1} = \left( \frac{M_{1+2}}{M_1} \right) \left( \frac{\sigma_1^2}{\sigma_{1+2}^2} \right) \approx \left( \frac{M_{1+2}}{M_1} \right)^2. \quad (10)$$

The effective radius grows by the square of the change in mass (rather than linearly, which is the case for equal-mass mergers) and the velocity dispersion decreases by the square root of the change in mass (rather than remaining constant) (see also Naab et al. 2009). As an example, eight successive  $M_2 : M_1 = 1 : 10$  mergers could lead to a factor of  $\sim 5$  increase in effective radius, while the mass would grow by a factor of  $\sim 2$  only.

The effects of this scenario are shown by the green arrows in Fig. 2. Again, the density within 1 kpc was calculated by assuming that the Sersic index of the profiles remains unchanged. The compact galaxies have a median mass of  $1.7 \times 10^{11} M_\odot$  therefore the minor merger model predicts that their descendants are in galaxies with a median mass of  $3-4 \times 10^{11} M_\odot$  today. The central densities of these galaxies are a very good match to those of the predicted descendants (panel *d*), and the effective radii are a much better match than in the equal-mass merger model (panel *a*). We note here that what matters is the direction of the arrows, as their length is arbitrarily determined by a growth of a factor of five in  $r_e$ . Extending the green arrows slightly would bring them very close to the distribution of nearby elliptical galaxies in all panels.

##### 4.3. Model 3: Expansion at Fixed Mass

In the final model that we examine, a galaxy has accumulated most of its mass by  $z \sim 2$  and then gradually expands over time while its mass stays roughly constant. The motivation for this class of models was provided by Fan et al. (2008); they suggest that a QSO may blow out a large fraction of the mass, leading to a significant “puffing up” of the remnant. We will discuss whether such models are physically plausible in § 5.2 (see also Trujillo et al. 2009).

Predictions for these models are indicated by red arrows in Fig. 2. By construction, these models predict the right amount of size evolution at fixed mass, and therefore produce the same values of  $\rho(< r_e)$  as nearby elliptical galaxies. However, as can be seen in panels *b* and *d* they slightly under-predict the central densities of local ellipticals. The values of  $\rho(< 1 \text{ kpc})$  that are predicted are a factor of  $\sim 2$  lower than those of local ellipticals with the same mass.

##### 4.4. Summary of Model Comparisons

We conclude that all three simple models bring the compact galaxies much closer to the relations defined by nearby elliptical galaxies. The equal-mass merger model provides the worst description of the three as it does not produce elliptical galaxies of the right size and is therefore probably not the dominant mode of growth. The minor merger is more effective in puffing up the compact galaxies and, despite its simplicity, provides a remarkably good description of the masses and densities of nearby elliptical galaxies. The expansion model provides a good description as well, although it slightly under-predicts the central densities of elliptical galaxies.

## 5. DISCUSSION

The main result of the previous Section, and this paper, is that the properties of high redshift compact galaxies can be reconciled with those of nearby massive elliptical galaxies. The densities of the compact galaxies are similar to the central densities of elliptical galaxies, and simple “toy models” can be used to describe the evolution.

### 5.1. Independent Constraints on Mass Growth

The amount of mass growth in the models of § 4 is specified by the physical mechanism for growth (equal-mass merger, minor mergers, and expansion) and the choice of a factor of five increase in effective radius. To achieve this increase, the equal-mass merger model requires an increase in mass of a factor of  $\sim 5$ , the minor merger model requires an increase of a factor of 2–3, and the expansion model does not require an increase at all.

The evolution of the galaxy mass function provides an independent constraint on the mass growth. The compact galaxies are common at the epoch of observation – they constitute  $\gtrsim 90\%$  of “red and dead” galaxies at  $z = 2.3$  (vD08) and therefore some  $\sim 50\%$  of the general population of galaxies with stellar masses  $\gtrsim 10^{11} M_{\odot}$  (e.g., Kriek et al. 2006; Kriek et al. 2008; Williams et al. 2008). The evolution of the galaxy mass function has been measured recently by several groups (e.g., Drory et al. 2005; Fontana et al. 2006; Marchesini et al. 2008; Pérez-González et al. 2008). Here, we use the results from Marchesini et al. (2008), who have combined data from both deep and wide surveys in a self-consistent way. Integrating the Schechter function fit given in Marchesini et al. (2008) we find that the integrated number density of galaxies with stellar masses  $M > 10^{11} M_{\odot}$  is  $7.2_{-1.1}^{+1.1} \times 10^{-5} \text{ Mpc}^{-3}$  at  $z = 2.5$ . The number density of compact, quiescent galaxies is therefore  $3.6_{-0.9}^{+0.9} \times 10^{-5} \text{ Mpc}^{-3}$ , where we assumed that the quiescent fraction is  $0.5 \pm 0.1$ . The stellar mass density in these galaxies is  $4.8_{-1.9}^{+1.6} \times 10^6 M_{\odot} \text{ Mpc}^{-3}$ .

This number density and mass density provide strict bounds on the typical masses of the descendants of the compact galaxies. If the mass density of the compact galaxies exceeds that of local galaxies of a particular mass it is immediately clear that these local galaxies cannot constitute the (sole) descendants. Figure 3 shows the integrated Schechter stellar mass function in the local universe in dark grey, as well as the number density of compact galaxies with  $M > 10^{11} M_{\odot}$  at  $z = 2.5$  in light grey. For any descendant population at  $z = 0.1$ , mass corresponds to a required growth factor, given on the lower axis. We first ignore mergers of compact galaxies with themselves and address that possibility later. In order for a model to be a feasible evolutionary path the implied descendant population of galaxies in the local universe must be at least as common as the progenitors at high redshift.

The number density of nearby massive galaxies limits the mass growth to a factor of 2–3. For this mass growth each compact galaxy has one descendant. Lower mass growth implies that only a small fraction of massive galaxies today hosts a descendant of a compact galaxy. Higher mass growth is not allowed, as it would create too many descendants. Of course, these constraints are dependent on the masses at  $z = 2.5$ , which we derived. If these masses are incorrect, this argument might change.

Vertical lines in Fig. 3 indicate predictions from the three models discussed in § 4. The expansion model is obviously fully consistent with the constraints imposed by the evolution

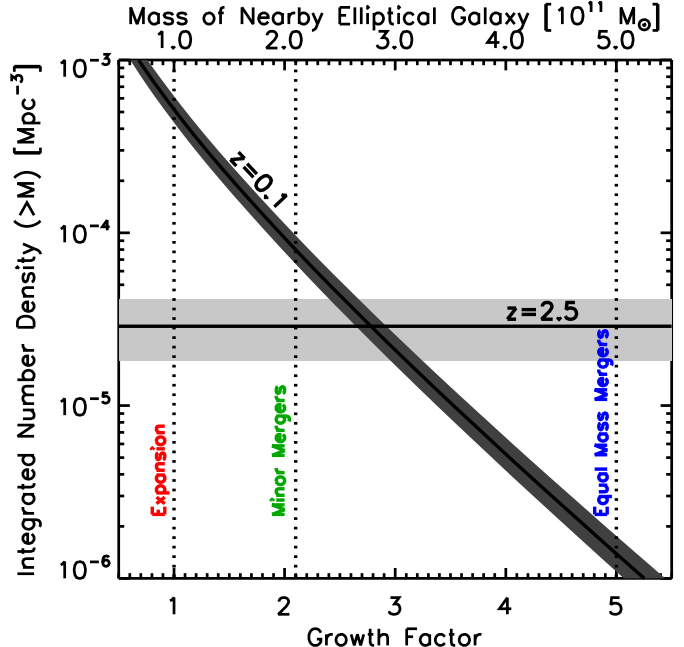


FIG. 3.— Integrated number density of galaxies above a mass limit. The horizontal line is the number density of quiescent galaxies with  $M > 10^{11} M_{\odot}$  at  $z = 2.5$ . The diagonal relation is the number density at low redshift as a function of the mass limit. The mass limit is indicated in absolute units on the top axis, and as a growth factor compared to  $z = 2.5$  on the bottom axis. Vertical lines indicate the growth implied by the simple models discussed in § 4. Ignoring merging of compact galaxies with themselves, the mass functions at  $z = 2.5$  and  $z \sim 0$  do not allow for growth of more than a factor of 2–3. Strong merging of compact galaxies is ruled out by the integrated mass density at low redshift (see text).

of the mass function, as it implies no mass growth. We note that only  $\sim 7\%$  of nearby galaxies with masses  $> 10^{11} M_{\odot}$  are descendants of quiescent  $z = 2.5$  galaxies in this model; we will return to this point below. Remarkably, we can rule out the equal-mass merger model as the main mode of growth based on Fig. 3, as it implies a mass growth of a factor of  $\sim 5$ . The number density of nearby galaxies with  $M > 5 \times 10^{11} M_{\odot}$  is lower by more than an order of magnitude than the number density of compact galaxies with  $M > 10^{11} M_{\odot}$  at  $z = 2.5$ . In the equal-mass merger model, compact galaxies can obviously merge with each other, which will lower their number density. However, a factor of  $\sim 5$  mass growth is not allowed even when compact galaxies are *only* permitted to merge with each other: the stellar mass density in galaxies with  $M > 5 \times 10^{11} M_{\odot}$  at  $z = 0.1$  is  $8.1_{-1.6}^{+2.1} \times 10^5 M_{\odot} \text{ Mpc}^{-3}$ , a factor of 6 lower than the mass density in compact galaxies with  $M > 10^{11} M_{\odot}$  at  $z = 2.5$ .

Also remarkably, the growth in the minor merger model is close to the cross-over point, where each compact galaxy has one descendant. A plausible explanation is that the central parts of many elliptical galaxies formed at  $z > 2.5$ , after which they grew through minor, mostly dry mergers.

More generally, we can combine panel *a* of Fig. 2 with Fig. 3 to derive an empirical constraint on the amount of size growth for a given amount of mass growth. Parameterizing the relation between size growth and mass growth as

$$\frac{r_{1+2}}{r_1} = \left( \frac{M_{1+2}}{M_1} \right)^{\alpha}, \quad (11)$$

we find that  $\alpha \gtrsim 2$  to simultaneously satisfy the constraints from the evolution of the size – mass relation (Fig. 2a; van der Wel et al. 2008), and from the evolution of the mass func-

tion. This limit for  $\alpha$  is similar to naive expectations from minor mergers, which is why we obtain a good correspondence between progenitors and descendants for this class of models. The equal-mass merger model has  $\alpha \sim 1$  (or even  $< 1$ ; see Boylan-Kolchin et al. 2006); for the expansion model  $M_{1,f}/M_1 = 1$  (or even  $< 1$ ) and Eq. 11 is not well defined.

### 5.2. Which Models are Physically Plausible?

We expect that each of these toy models is responsible at some level for the growth and evolution of galaxies from  $z \sim 2.5$  until today. Observational evidence of merging events, both equal-mass and minor, exists at intermediate redshifts and can definitely produce growth in galaxy mass and size. Mass loss from the central regions of galaxies should also occur and would therefore cause increases in galaxy sizes. Given this complexity, we hope to identify which of our simple models best describes the mechanism responsible for the majority of the growth of the compact galaxies at high redshifts into descendant galaxies in the nearby universe.

In § 5.1 we found that the equal-mass merger model is inconsistent with the number density of massive galaxies today. We are therefore left with two feasible models, growth via “in-situ” expansion or via minor mergers. Both of these modes of galaxy growth have the effect of puffing up the galaxies without extreme mass growth. Number densities of the implied descendants of galaxies that have grown via either mode correspond to sufficiently common galaxies in the local universe.

Although number density arguments do not immediately discredit the expansion model of galaxy evolution, they do lead to uncomfortable questions. The implication of no mass growth is that only a very small number of nearby galaxies with mass  $> 10^{11} M_\odot$  was already formed at  $z = 2.5$ : approximately 7 % if only quiescent galaxies at  $z = 2.5$  are considered, and  $\sim 14$  % if all galaxies with  $M > 10^{11} M_\odot$  are considered. This raises the question where the progenitors of the remaining  $\sim 90$  % of today’s massive galaxies are at  $z = 2.5$ . In a hierarchical growth scenario, one expects that the most massive galaxies today have always been the most massive galaxies. Instead, the expansion model implies that the most massive galaxies at  $z \sim 2.5$  evolve into a small fraction of average-mass elliptical galaxies today. Furthermore, the most massive galaxies in the local universe, with masses  $M \gtrsim 3 \times 10^{11} M_\odot$  must then have formed rapidly in the later universe, implying an extremely active merging history of smaller objects. One might conclude that they formed through star formation at lower redshift, but this would be inconsistent with the stellar ages of massive ellipticals (e.g., Thomas et al. 2005; van Dokkum 2008).

There are other potential problems with the physical model proposed by Fan et al. (2008). The growth relies on strong heating of the inner regions of the galaxy, such as that produced by a central active galactic nucleus (AGN). However, the high redshift galaxies in our sample are already shown to be quiescent, with old stellar populations. If there was an active central engine at one point in the galaxies’ histories, it would have already blown out gas and led to expansion of the galaxy. While growth through mass loss may have played a role in the evolution of such galaxies, it is unlikely to do so again between  $z = 2.5$  and  $z = 0$ , except possibly through stellar winds and supernovae. Based on simulations of open clusters, Fan et al. (2008) argue that there could be a long delay between the expulsion of gas and the response of the stellar distribution to the new potential, but it is not clear whether these simulations can easily be applied to massive galaxies.

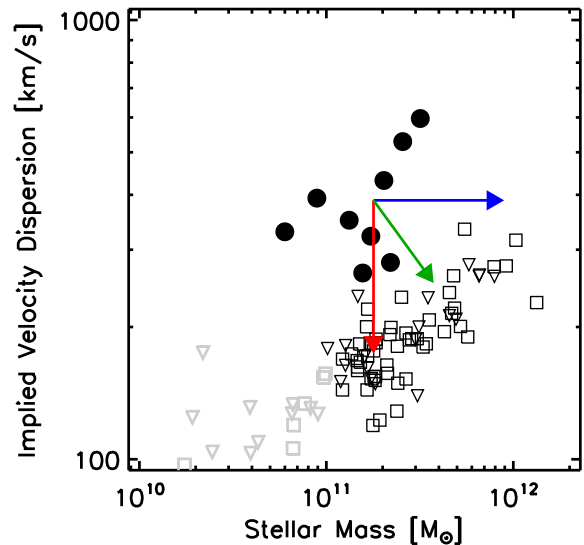


FIG. 4.— Implied velocity dispersions of high and low redshift galaxies, along with approximate predictions from the three models discussed in § 4.

Finally, the expansion model requires significant fine-tuning of the amount of mass that is removed from the galaxies: removing a small fraction of the mass does not have an appreciable effect, and removing too much would destroy the galaxies.

Minor mergers (or rather, “un-equal mass mergers”) are expected in galaxy formation models, and are predicted to dominate the mass growth of massive galaxies at late times (e.g., Naab et al. 2007; Guo & White 2008). Simulations have shown that the central regions of a galaxy can be minimally affected by dry mergers but that an envelope of newly accreted material is formed that grows with time (Naab et al. 2007). They have also been observed (e.g., Schweizer & Seitzer 1992). van Dokkum (2005) infers that visible tidal features around nearby elliptical galaxies are caused by red mergers with median mass ratio 1 : 4. It is an open question whether the merger rate is sufficiently high to produce a factor of 2–3 growth in mass since  $z = 2.5$ . Models do predict high accretion rates (e.g., De Lucia et al. 2006; Naab et al. 2007; Guo & White 2008), but some observations suggest that mass growth may be small for the highest masses (e.g., Cool et al. 2008).

Minor merger models are also qualitatively consistent with the uniform and gradual evolution of the size – mass relation (e.g., Franx et al. 2008; van der Wel et al. 2008), and the apparent lack of old massive compact galaxies in the local Universe (e.g., Trujillo et al. 2009). If equal-mass mergers were a dominant mechanism one might expect to find some galaxies that did not experience a major merger and are therefore left intact at the present day, but this is very unlikely in a minor merger model.

### 5.3. Implied Velocity Dispersions

As has been pointed out in several studies, the small sizes and high masses of the compact red galaxies imply very high velocity dispersions (Toft et al. 2007; Cimatti et al. 2008; van Dokkum et al. 2008). Figure 4 demonstrates the implied dynamical properties of the nearby and high redshift galaxy population as well as the possible evolutionary tracks of these

galaxies.

We calculated the velocity dispersions from the equation given in van Dokkum & Stanford (2003):

$$\log M \equiv 2 \log \sigma + \log r_e + 6.07, \quad (12)$$

with  $r_e$  in kpc and  $M$  in Solar masses. This expression is not very accurate as it does not take the relation between  $M$  and  $M/L$  or the effects of a dark halo into account, but it does allow a comparison in a self-consistent way.

Predictions from the simple models of § 4 are shown by arrows. The expansion model predicts that the dispersions decrease over time, as the total mass of the galaxy remains constant and the effective radius increases. As discussed in § 4.1 the equal-mass merger model predicts that the velocity dispersions remain constant as the mass grows, which implies that the descendants have velocity dispersions that are higher than are implied by the galaxies in the local sample. Growth by minor mergers presents a possible method of decreasing the velocity dispersion of the galaxies, as the expansion is a stronger factor than mass growth. This mechanism, again shown by the green arrow on Figure 4(a), evolves the compact galaxies onto the velocity dispersion trend for local galaxies. This assumes mass growth by a factor of 2.1, based on the same specific minor merging history described in § 4.2, and size growth by a factor of 5.

## 6. SUMMARY AND CONCLUSIONS

The main result from our study is that nearby elliptical galaxies have similar average densities within 1 kpc as the recently discovered compact “red and dead” galaxies at high redshift. The descendants of the compact “red and dead” galaxies at  $z > 2$  could therefore simply constitute the central parts of today’s massive elliptical galaxies.

Models dominated by minor mergers (where “minor” implies “not equal mass”) can increase the sizes of the galaxies efficiently, without violating constraints from the evolution of the evolution of the mass function as measured by Marchesini et al. (2008). Interestingly, the evolution of the mass – size relation and the mass function together imply that  $\sim 50\%$ <sup>5</sup> of elliptical galaxies with mass  $\gtrsim 2 - 3 \times 10^{11} M_\odot$  may have the remnant of a compact  $z = 2.5$  galaxy with mass  $\gtrsim 1 \times 10^{11} M_\odot$  in its center. Models which require energy input by a central engine to “puff up” the galaxies can also adequately evolve compact galaxies into sufficiently common local counterparts, but these models require significant fine-tuning and may not be physically plausible as the primary growth mechanism. We note that we did not consider star formation as a way to grow the compact  $z \sim 2.3$  galaxies. Although it is possible that star formation re-starts at lower redshifts, newly formed stars can only account for a small fraction of the final mass given the stellar ages inferred for massive ( $\gtrsim 2 \times 10^{11} M_\odot$ ) galaxies at  $z = 0$  (e.g., Thomas et al 2005, van Dokkum & van der Marel 2007). Nevertheless, a small amount of star formation could help increase the sizes between  $z \sim 2.3$  and  $z = 0$  (see also Franx et al. 2008).

The minor merger model predicts evolution in the Magorrian et al. (1998) relation between black hole mass and velocity dispersion. The central black hole will grow from  $z = 2.3$  to the present, with the amount of growth determined by the black hole masses of the infalling galaxies. However, the ve-

locity dispersion will decrease by a factor of  $\sim 1.5$ . Therefore, even if the black hole growth is insignificant, black hole masses at fixed velocity dispersion will be significantly lower at  $z \sim 2.5$  than at  $z = 0$ . Robertson et al. (2006b) came to the same conclusion using merger simulations, but this prediction contrasts with several other studies (e.g., Cen 2007; Woo et al. 2008).

The galaxy growth models that we describe here are simple and the empirical findings are preliminary, highlighting the need for further study. On the modeling side, the main uncertainties are whether the merger rate is sufficiently high to produce the required growth, and whether a realistic treatment of the dark matter and orbital configurations retains the high efficiency of minor mergers to “puff up” a galaxy. Whatever the dominant physical mechanism turns out to be, we find that  $\alpha \gtrsim 2$  if the relation between size growth and mass growth is parameterized as  $r_{1+2}/r_1 = (M_{1+2}/M_1)^\alpha$ .

Inside-out formation via mergers predicts that stars in the central regions of a nearby elliptical galaxy are qualitatively different from stars at larger radii. Elliptical galaxies do have color- and metallicity gradients, which could reflect differences in stellar populations between stars formed in-situ and those accreted from other systems (e.g., Peletier et al. 1990). While it is not yet clear whether these gradients are consistent with such accretion scenarios, it may be difficult to reconcile them with an expansion model alone (see, e.g., Pipino & Matteucci 2008). It is tempting to identify kinematically decoupled cores (e.g., Franx & Illingworth 1988; Bender 1988) with the descendants of the compact galaxies, but the scales of these features are typically a few 100 pc rather than  $\sim 1$  kpc. More information on color gradients and the inner  $\sim 1$  kpc of the compact high redshift galaxies will provide important additional constraints.

Our determinations of stellar density profiles and masses can be improved. The calculated density profiles and integrated masses are based on Sersic profile fits to the galaxy light distributions, not on the actual light profiles themselves. Furthermore, for the high redshift galaxies the profiles within  $\sim 1$  kpc are extrapolations, as the galaxies are not resolved on smaller scales. The conversion from light to mass is also very uncertain. The conversion for the local samples ignores scatter in the  $M/L$  versus  $L$  relation, and ignores gradients in  $M/L$  ratio. The mass estimates of the high redshift galaxies are based on stellar population models and are very sensitive to the assumed IMF and to possible contributions from dark matter. As noted in § 1, bottom-light IMFs would change the masses and alter the required amount of size- and mass evolution to bring the galaxies to local relations.

Measurements of absorption-line kinematics of high redshift compact galaxies would provide a direct test of the IMF, and of several of the other assumptions that enter the analysis (see, e.g., Cimatti et al. 2008). van der Wel et al. (2008) find that the observed size evolution at  $0 < z < 1$  is similar when dynamical masses rather than photometric masses are used, but this needs to be verified at higher redshifts.

We thank Avishai Dekel and Jeremiah Ostriker for helpful discussions. Support from NASA grants HST-GO-10808 and HST-GO-10809 is gratefully acknowledged.

<sup>5</sup> In a minor merger model the exact fraction could range from  $\sim 10\%$  –  $\sim 100\%$ , depending on the order and mass ratio of mergers.

## REFERENCES

Barnes, J. E. 1992, *ApJ*, 393, 484  
 Bender, R. 1988, *A&A*, 202, L5  
 Bournaud, F., Jog, C. J., & Combes, F. 2007, *A&A*, 476, 1179  
 Boylan-Kolchin, M., Ma, C.-P., & Quataert, E. 2006, *MNRAS*, 353  
 Buitrago, F., Trujillo, I., Conselice, C. J., Bouwens, R. J., Dickinson, M., Yan, H., et al. 2008, *ApJ*, 687, L61  
 Cen, R. 2007, *ApJ*, 654, L37  
 Cimatti, A., Cassata, P., Pozzetti, L., Kurk, J., Mignoli, M., Renzini, A., Daddi, E., Bolzonella, M., et al. 2008, *A&A*, 482, 21  
 Ciotti, L. 1991, *A&A*, 249, 99  
 Ciotti, L., & Bertin, G. 1999, *A&A*, 352, 447  
 Cool, R. J., Eisenstein, D. J., Fan, X., Fukugita, M., Jiang, L., Maraston, C., Meiksin, A., Schneider, D. P., et al. 2008, *ApJ*, 682, 919  
 Daddi, E., Renzini, A., Pirzkal, N., Cimatti, A., Malhotra, S., Stiavelli, M., Xu, C., Pasquali, A., et al. 2005, *ApJ*, 626, 680  
 Damjanov, I., McCarthy, P. J., Abraham, R. G., Glazebrook, K., Yan, H., Mentuch, E., Le Borgne, D., Savaglio, S., et al. 2008, ArXiv e-prints  
 Davé, R. 2008, *MNRAS*, 385, 147  
 De Lucia, G., Springel, V., White, S. D. M., Croton, D., & Kauffmann, G. 2006, *MNRAS*, 366, 499  
 Dekel, A., Birnboim, Y., Engel, G., Freundlich, J., Goerdt, T., Mumcuoglu, M., Neistein, E., Pichon, C., et al. 2008, ArXiv e-prints  
 Drory, N., Salvato, M., Gabasch, A., Bender, R., Hopp, U., Feulner, G., & Pannella, M. 2005, *ApJ*, 619, L131  
 Fan, L., Lapi, A., De Zotti, G., & Danese, L. 2008, *ApJ*, 689, L101  
 Fontana, A., Salimbeni, S., Grazian, A., Giallongo, E., Pentericci, L., Nonino, M., Fontanot, F., Menci, N., et al. 2006, *A&A*, 459, 745  
 Franx, M., Illingworth, G., & Heckman, T. 1989, *AJ*, 98, 538  
 Franx, M., & Illingworth, G. D. 1988, *ApJ*, 327, L55  
 Franx, M., van Dokkum, P. G., Schreiber, N. M. F., Wuyts, S., Labb  , I., & Toft, S. 2008, *ApJ*, 688, 770  
 Guo, Q., & White, S. D. M. 2008, *MNRAS*, 384, 2  
 Hopkins, P. F., Hernquist, L., Cox, T. J., Keres, D., & Wuyts, S. 2008, ArXiv e-prints  
 Jedrzejewski, R. I. 1987, *MNRAS*, 226, 747  
 Khochfar, S., & Silk, J. 2006, *ApJ*, 648, L21  
 Kriek, M., van Dokkum, P. G., Franx, M., Illingworth, G. D., Marchesini, D., Quadri, R., Rudnick, G., Taylor, E. N., et al. 2008, *ApJ*, 677, 219  
 Kriek, M., van der Wel, A., van Dokkum, P. G., Franx, M., Illingworth, G. D., et al. 2008, *ApJ*, 682, 896  
 Kriek, M., van Dokkum, P. G., Franx, M., Quadri, R., Gawiser, E., Herrera, D., Illingworth, G. D., Labb  , I., et al. 2006, *ApJ*, 649, L71  
 Kroupa, P. 2001, *MNRAS*, 322, 231  
 Loeb, A., & Peebles, P. J. E. 2003, *ApJ*, 589, 29  
 Magorrian, J., Tremaine, S., Richstone, D., Bender, R., Bower, G., Dressler, A., Faber, S. M., Gebhardt, K., et al. 1998, *AJ*, 115, 2285  
 Marchesini, D., van Dokkum, P. G., Forster Schreiber, N. M., Franx, M., Labb  , I., & Wuyts, S. 2008, ArXiv e-prints  
 Naab, T., Johansson, P. H., Ostriker, J. P., & Efstathiou, G. 2007, *ApJ*, 658, 710  
 Naab, T., Johansson, P. H., & Ostriker, J. P. 2009, submitted  
 Peletier, R. F., Davies, R. L., Illingworth, G. D., Davis, L. E., & Cawson, M. 1990, *AJ*, 100, 1091  
 Peng, C. Y., Ho, L. C., Impey, C. D., & Rix, H.-W. 2002, *AJ*, 124, 266  
 P  rez-Gonz  lez, P. G., Rieke, G. H., Villar, V., Barro, G., Blaylock, M., Egami, E., Gallego, J., Gil de Paz, A., et al. 2008, *ApJ*, 675, 234  
 Pipino, A., & Matteucci, F. 2008, *A&A*, 486, 763  
 Prugniel, P., & Heraudeau, P. 1998, *A&AS*, 128, 299  
 Robertson, B., Cox, T. J., Hernquist, L., Franx, M., Hopkins, P. F., Martini, P., & Springel, V. 2006a, *ApJ*, 641, 21  
 Robertson, B., Hernquist, L., Cox, T. J., Di Matteo, T., Hopkins, P. F., Martini, P., & Springel, V. 2006b, *ApJ*, 641, 90  
 Schlegel, D. J., Finkbeiner, D. P., & Davis, M. 1998, *ApJ*, 500, 525  
 Schweizer, F., & Seitzer, P. 1992, *AJ*, 104, 1039  
 Sersic, J. L. 1968, *Atlas de galaxias australes* (Cordoba, Argentina: Observatorio Astronomico, 1968)  
 Tal, T., van Dokkum, P. G., Nelan, J., & Bezzanson, R. 2009, in preparation  
 Thomas, D., Maraston, C., Bender, R., & Mendes de Oliveira, C. 2005, *ApJ*, 621, 673  
 Toft, S., van Dokkum, P., Franx, M., Labb  , I., F  rster Schreiber, N. M., Wuyts, S., Webb, T., Rudnick, G., et al. 2007, *ApJ*, 671, 285  
 Trujillo, I., Cenarro, A. J., de Lorenzo-Caceres, A., Vazdekis, A., de la Rosa, I. G., & Cava, A. 2009, ArXiv e-prints  
 Trujillo, I., F  rster Schreiber, N. M., Rudnick, G., Barden, M., Franx, M., Rix, H.-W., Caldwell, J. A. R., McIntosh, D. H., et al. 2006, *ApJ*, 650, 18  
 Tully, R. B. 1988, *Nearby galaxies catalog* (Cambridge and New York, Cambridge University Press, 1988, 221 p.)  
 van der Marel, R. P. 1991, *MNRAS*, 253, 710  
 van der Marel, R. P., & van Dokkum, P. G. 2007, *ApJ*, 668, 756  
 van der Wel, A., Holden, B. P., Zirm, A. W., Franx, M., Rettura, A., Illingworth, G. D., & Ford, H. C. 2008, *ApJ*, 688, 48  
 van Dokkum, P. G. 2005, *AJ*, 130, 2647  
 —. 2008, *ApJ*, 674, 29  
 van Dokkum, P. G., & Franx, M. 2001, *ApJ*, 553, 90  
 van Dokkum, P. G., Franx, M., Kriek, M., Holden, B., Illingworth, G. D., Magee, D., Bouwens, R., Marchesini, D., et al. 2008, *ApJ*, 677, L5  
 van Dokkum, P. G., Quadri, R., Marchesini, D., Rudnick, G., Franx, M., Gawiser, E., Herrera, D., Wuyts, S., et al. 2006, *ApJ*, 638, L59  
 van Dokkum, P. G., & Stanford, S. A. 2003, *ApJ*, 585, 78  
 White, M., Zheng, Z., Brown, M. J. I., Dey, A., Jannuzzi, B. T., et al. 2007, *ApJ*, 655, L69  
 Wilkins, S. M., Trentham, N., & Hopkins, A. M. 2008, *MNRAS*, 385, 687  
 Williams, R. J., Quadri, R. F., Franx, M., van Dokkum, P., & Labb  , I. 2008, ArXiv e-prints  
 Woo, J.-H., Treu, T., Malkan, M. A., & Blandford, R. D. 2008, *ApJ*, 681, 925  
 Zirm, A. W., van der Wel, A., Franx, M., Labb  , I., Trujillo, I., van Dokkum, P., Toft, S., Daddi, E., et al. 2007, *ApJ*, 656, 66